56. *Deformation of the Earth's Crust in Idu Peninsula in Connection with the Destructive Idu Earthquake of Nov. 26, 1930.*

By Seiti YAMAGUTI,

Earthquake Research Institute.

(Read March 16, 1937.—Received. Sept. 20, 1937.)

C. Tsuboi[1] has already studied the deformation of the earth's crust in the regions that were severely disturbed by the Idu destructive earthquake of Nov. 26, 1930. Since, at the time of his study, horizontal displacements caused by the earthquake of only 13 second-order trigonometrical points in the regions were available, detailed discussion was impossible. The object of the present paper is to discuss the same problem in greater detail using as data the horizontal and vertical displacements of 71 third-order trigonometrical points in this region which have been measured and placed at our disposal recently by the Military Land Survey. It is hoped to find some physical relationship between the vertical and horizontal displacements of the earth's crust.

The displacements of the trigonometrical points to be discussed were derived from comparisons of their geographical positions after the Idu earthquake and those after the great Kwantô earthquake of 1923. With 71 observed values of eastward (u) and northward (v) components of the displacements, two diagrams indicating u- and v-contours were drawn. On each of these diagrams, two series of parallel lines were drawn with intervals of 2 km., of which the one in EW and the other in NS directions. The values of u anr v at intersections of the lines were estimated by interpolation. In Fig. 1, the displacements of each of the mesh-points are shown by arrows, the heads of which are consecutively connected by straight lines in order that one may visualise the horizontal deformation of the earth's crust. A seismic fault, called the Tanna Fault, appeared at the time of the earthquake of 1930.

Referring to axes x and y, which were taken towards E and N, respectively, the values of $\frac{\partial u}{\partial x}$, $\frac{\partial u}{\partial y}$, $\frac{\partial v}{\partial x}$, and $\frac{\partial v}{\partial y}$ were calculated in the following way. Referring to the square shown in Fig. 2, which is one

1) C. TSUBOI, *Bull. Earthq. Res. Inst.*, 10 (1932), 435.

of a number of squares formed by two series of parallel lines, the

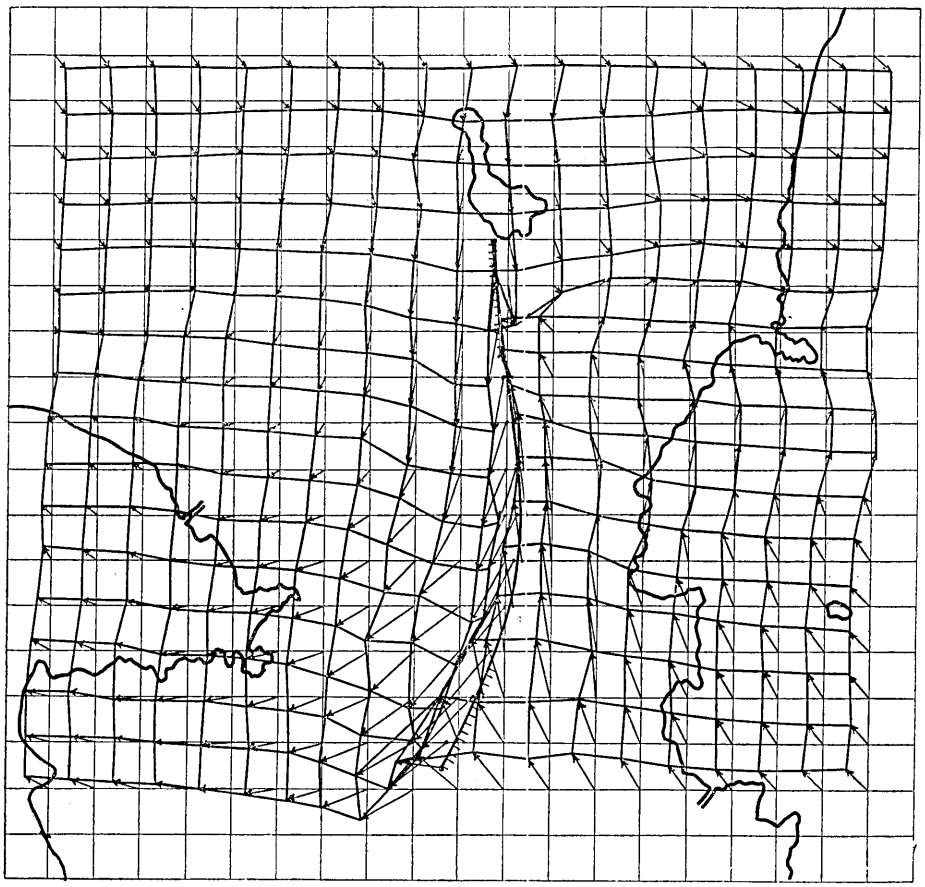

0 100 200 Cm Scale for Displacements.

Fig. 1. The Horizontal Displacements of the Mesh-points.

mean of $\frac{u_2-u_1}{2km}$ and $\frac{u_4-u_3}{2km}$ was taken to be the value of $\frac{\partial u}{\partial x}$ at the centre of the square. From the values of these and other horizontal gradients of horizontal displacements, which were calculated similarly, dilatation $\Delta=\frac{\partial u}{\partial x}+\frac{\partial v}{\partial y}$, shear $\sigma=\frac{1}{2}\left(\frac{\partial u}{\partial y}+\frac{\partial v}{\partial x}\right)$, and rotation $\omega=\frac{1}{2}\left(\frac{\partial u}{\partial y}-\frac{\partial v}{\partial x}\right)$ were obtained. The contour lines of these

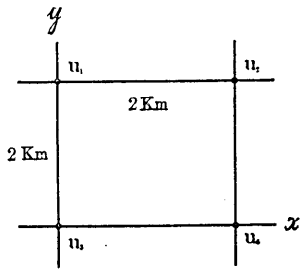

Fig. 2.

quantities are shown in Figs. 3 to 9. In *a* of each figure, the existence of the Tanna Seismic Fault, which is a line of discontinuity of dis-

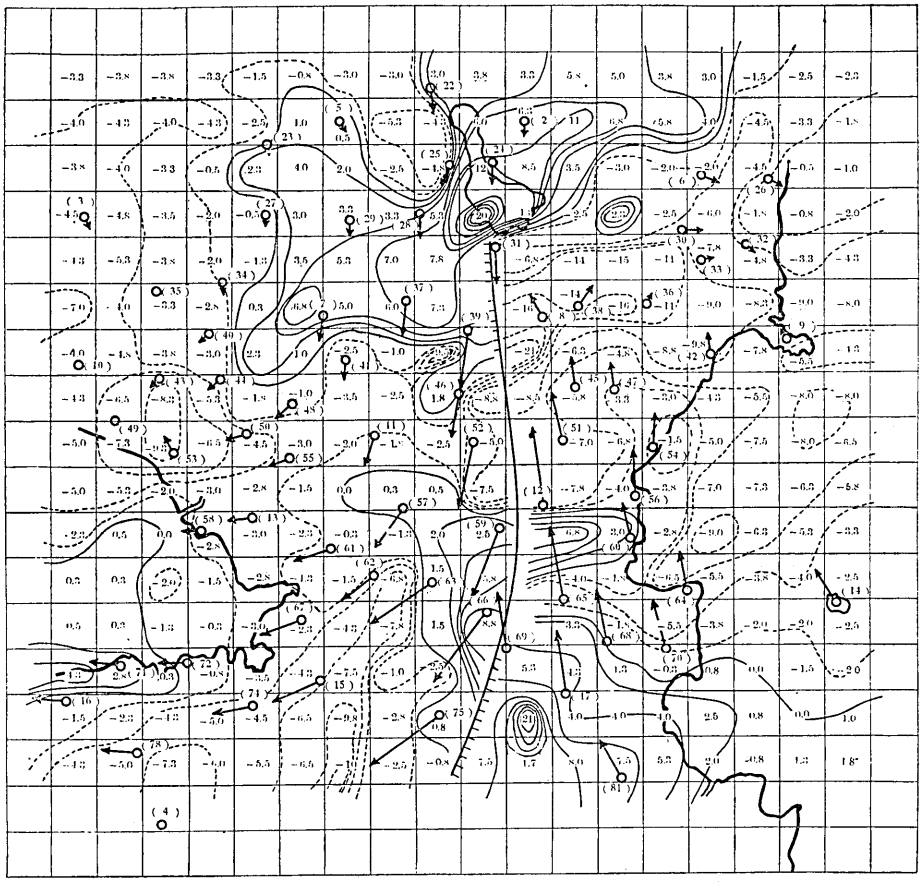

0 100 200 Cm

Scale for Displacements.

Fig. 3 *a*. Lines of Equal Dilatation,

$$\Delta=\frac{\partial u}{\partial x}+\frac{\partial v}{\partial y} \text{ in } 10^{-5}.$$

Arrows show the horizontal displacements of the Triangulation Points.

placement, was taken into consideration, while in *b* it is entirely ignored. The numerals in bracket in Fg. 3, *a*, correspond to the station numbers in Table 1.

Comparing the dilatation with vertical displacements, we see that regions of upheaval roughly agree in position with those of contraction, while regions of subsidence agree with those of dilatation. Since it seems from the geological structure of the regions that vertical displacement w may be more closely correlated with u, or $\frac{\partial u}{\partial x}$ than with

Table I.

Station number	Name of Station	Station number	Name of Station
2	Kamurigatake 冠ヶ岳	43	Nisisawata 西澤田
3	Asitakayama 愛鷹山	44	Okamiya 岡宮
5	Kamiyama 神山	45	Kunimiisi 國見石
6	Isibasi 石橋	46	Kuwabara 桑原
7	Sano 佐野	47	Idusan 伊豆山
8	Miyakami 宮上	48	Misimasiku 三島宿
9	Manaduru 眞鶴	49	Matunaga 松長
10	Negoya 根古屋	50	Ôoka 大岡
11	Ôba 大場	51	Hatamura 畑村
12	Kurodake 玄岳	52	Hirai 平井
13	Tokukurayama 德倉山	53	Numadu 沼津
14	Hasima 初島	54	$Atami_1$ 熱海一
15	Kosaka 小坂	55	Dôniwa 堂庭
16	Enasi 江梨	56	$Atami_2$ 熱海二
17	Sukumo 巢雲	57	Kasuya 柏谷
22	Otiai 落合	58	Simokanuki 下香貫
23	Kinesaka 木根坂	59	Nakoya 奈古谷
24	Wadanosumi 和田之角	60	Kamitaga 上多賀
25	Mikunitôge 三國峠	61	Himori 日守
26	Simoaido 下合戸	62	Yokkamati 四日町
27	Minamiyama 南山	63	Nirayama 韮山
28	Mihora 見洞	64	Aziro 網代
29	Yamasitairi 山下入	65	Simotaga 下多賀
30	Ôsawayama 大澤山	66	$Ukihasi_1$ 浮橋一
31	Umidaira 海平	67	Tozawa 戸澤
32	Minamiyosiwara 南吉原	68	$Usami_1$ 宇佐美一
33	Minamigô 南郷	69	$Ukihasi_2$ 浮橋二
34	Hatibudai 八分臺	70	$Usami_2$ 宇佐美二
35	Takayama 高山	71	Kuryô 久料
36	Uyeno 上野	72	Hirasawa 平澤
37	Suwadai 諏訪臺	73	Takyô 田京
38	Karesugi 枯杉	74	Sigesu 重須
39	Siroyama 城山	75	Ôno 大野
40	Nagasakadai 長坂臺	78	Kou 古宇
41	Kamohora 賀茂洞	79	Sizenzi 修善寺
42	Tatigakubo 立ヶ窪	81	Okamura 岡村

the dilatation, the contours of $\frac{\partial u}{\partial x}$, were compared with w, the contour of which last was drawn by the Military Land Survey, and shown in Fig. 10, *a*.

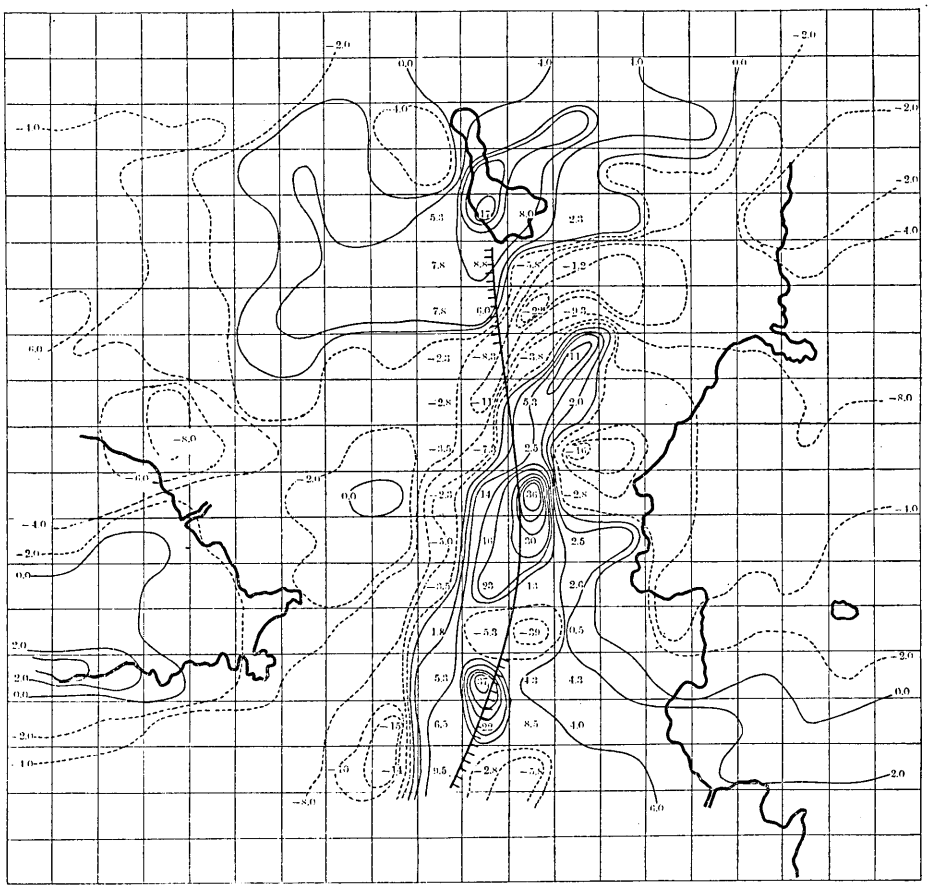

Fig. 3 *b*. Lines of Equal Dilatation,

$$\Delta=\frac{\partial u}{\partial x}+\frac{\partial v}{\partial y} \text{ in } 10^{-5}.$$

The existence of the Tanna Fault is entirely ignored.

The relation between u and w is shown in Fig. 10, b, in which the stations situated west of the Tanna Fault are indicated by O. The correlation coefficient between u and w is $-0{\cdot}38\pm0{\cdot}10$ if we take all points, and $-0{\cdot}57\pm0{\cdot}10$ if we take points only west of the fault. Thus correlation between u and w is especially close for points west of the Tanna Fault. Although nothing definite can be said for the points east of the Tanna Fault, a slight positive correlation seems to exist

between u and w. The correlation between u and w may be accounted for by the existence of a system of step-faults, along which parts of the earth's crust had slid as shown in Fig 11.

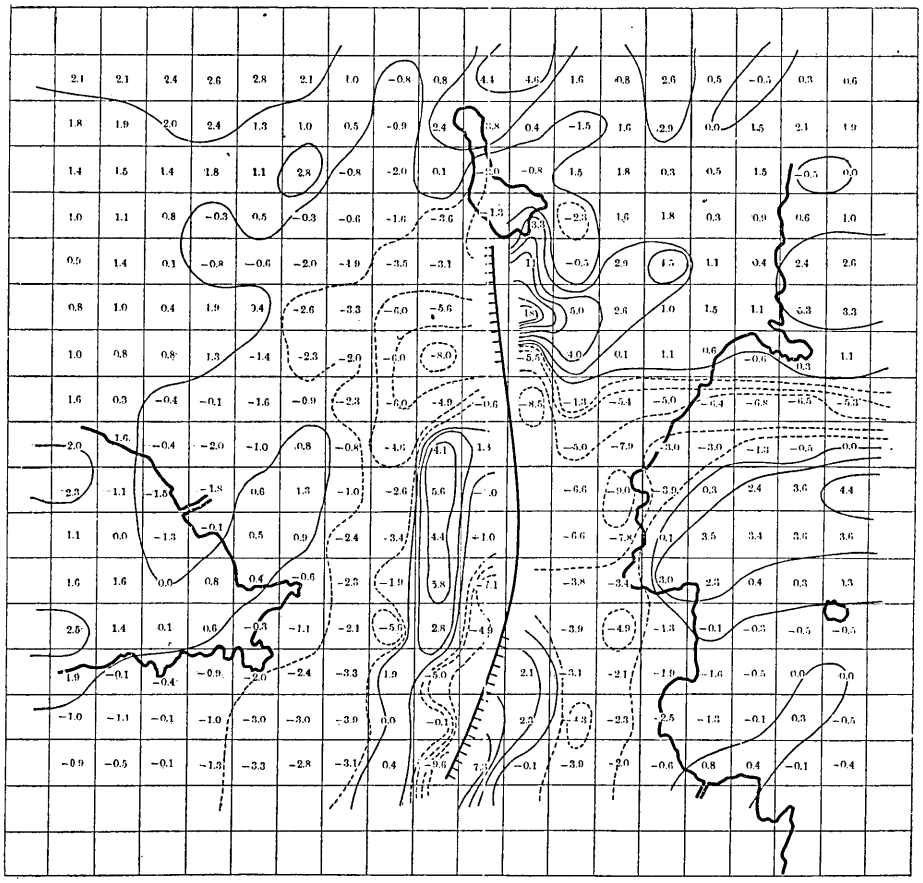

Fig. 4 *a*. Lines of Equal Shear,

$$\sigma=\frac{1}{2}\left(\frac{\partial u}{\partial y}+\frac{\partial v}{\partial x}\right) \text{ in } 10^{-5}.$$

The values of maximum shear $\sqrt{\left(\frac{\partial u}{\partial x}-\frac{\partial v}{\partial y}\right)^2+\left(\frac{\partial v}{\partial x}+\frac{\partial u}{\partial y}\right)^2}$, magnitudes γ, and directions θ, of the principal strains $\gamma_{1\,2}=\left(\frac{\partial u}{\partial x}+\frac{\partial v}{\partial y}\right)\pm\sqrt{\left(\frac{\partial u}{\partial x}-\frac{\partial v}{\partial y}\right)^2+\left(\frac{\partial v}{\partial x}+\frac{\partial u}{\partial y}\right)^2}$, and $\theta=\arctan\dfrac{\gamma_1-2\dfrac{\partial u}{\partial x}}{\dfrac{\partial u}{\partial y}+\dfrac{\partial v}{\partial x}}$ were calculated

and shown in Figs. 12, 18 respectively.

In order to ascertain the rate at which the magnitudes of the horizontal displacements u and v, and also those of dilatation, shear, rotation, and maximum shear, vary with distance from the Tanna Fault, the mean of their absolute values in zones parallel to the fault, which were taken every 2 km from it, were calculated. The values are plotted in Fig. 14, *a*, *b*, *c*, *d*, *e*, *f*, respectively.

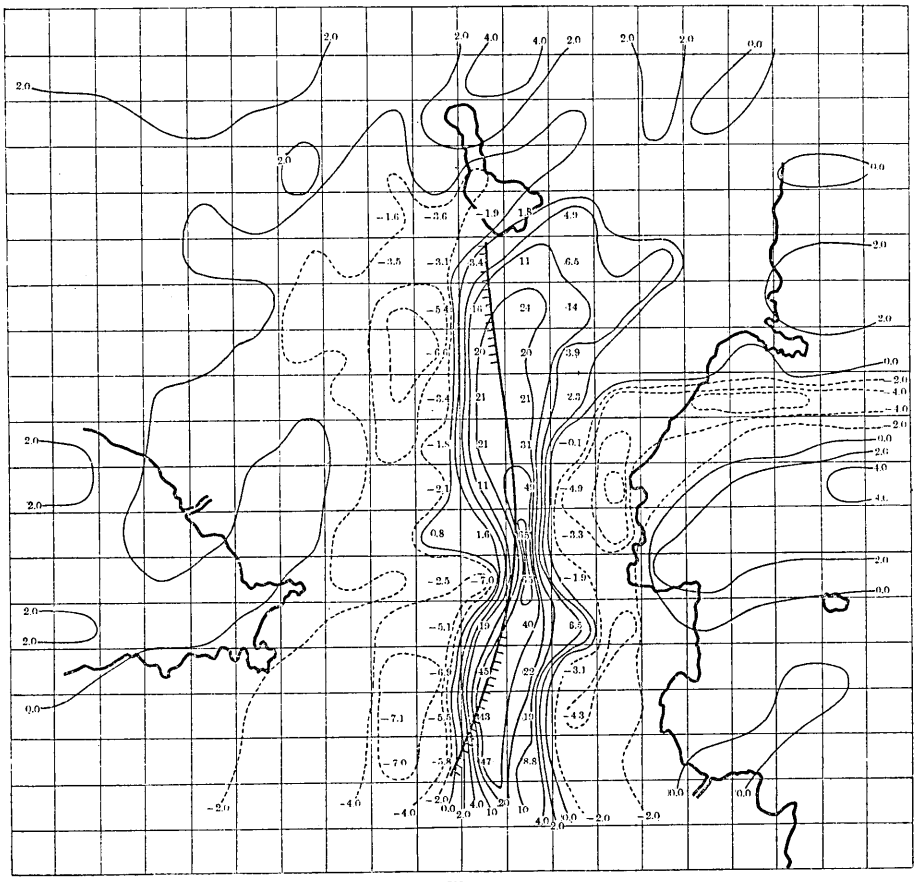

Fig. 4 *b*. Lines of Equal Shear,

$$\sigma=\frac{1}{2}\left(\frac{\partial u}{\partial y}+\frac{\partial v}{\partial x}\right) \text{ in } 10^{-5}.$$

The existence of the Tanna Fault is entirely ignored.

All the quantities here calculated are largest near the Tanna Fault, and decrease in magnitudes with distance from the fault, except, however, rotation and shear, which have conspicuous maxima at a distance of 6 km from the fault. As a rule, not only the horisontal displace-

ments u and v, but also dilatation, shear, rotation, and maximum shear too vague are all discontinuous across the fault line, and neither symmetry nor antisymmetry is to be seen east and west of the fault line.

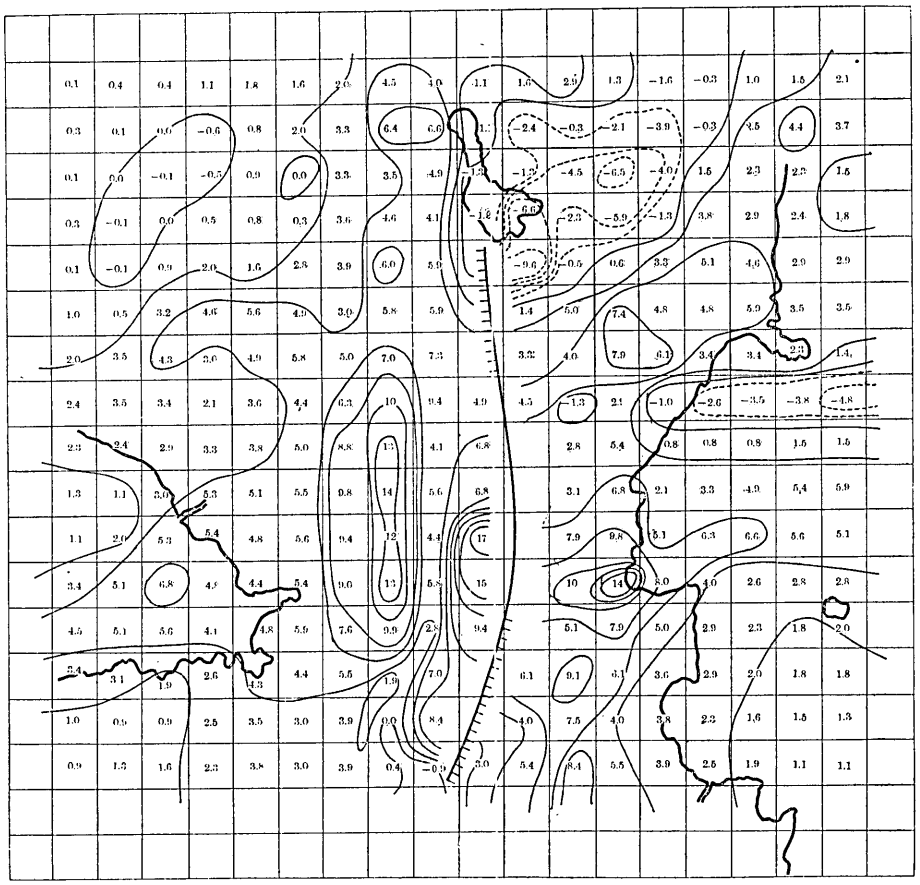

Fig. 5 *a*. Lines of Equal Rotation,

$$\omega=\frac{1}{2}\left(\frac{\partial u}{\partial y}-\frac{\partial v}{\partial x}\right) \text{ in } 10^{-5}.$$

A similar study was made of deformations of the earth's crust in Idu Peninsula, which are believed to have been connected in some way with the Great Kwantô Earthquake of Sept. 1, 1923. The results are shown in Figs. 15~24.

In this case, no distinct indication of the Tanna Fault can be seen, the large deformations of the earth's crust having mostly occurred in the vicinity of the epicentral region, i. e., about the northern coast of Sagami Bay. Thereas in the case of the Idu Destructive Earth-

quake, the vertical displacement w is negatively correlated with the eastward horizontal displacement u, in that of the Great Kwantô Earthquake we could see no definite correlation between them (the uw—diagram is omitted here).

Comparing the deformations of the earth's crust connected with (a) the Great Kwantô Earthquake and (b) the Idu Earthquake, we might say that

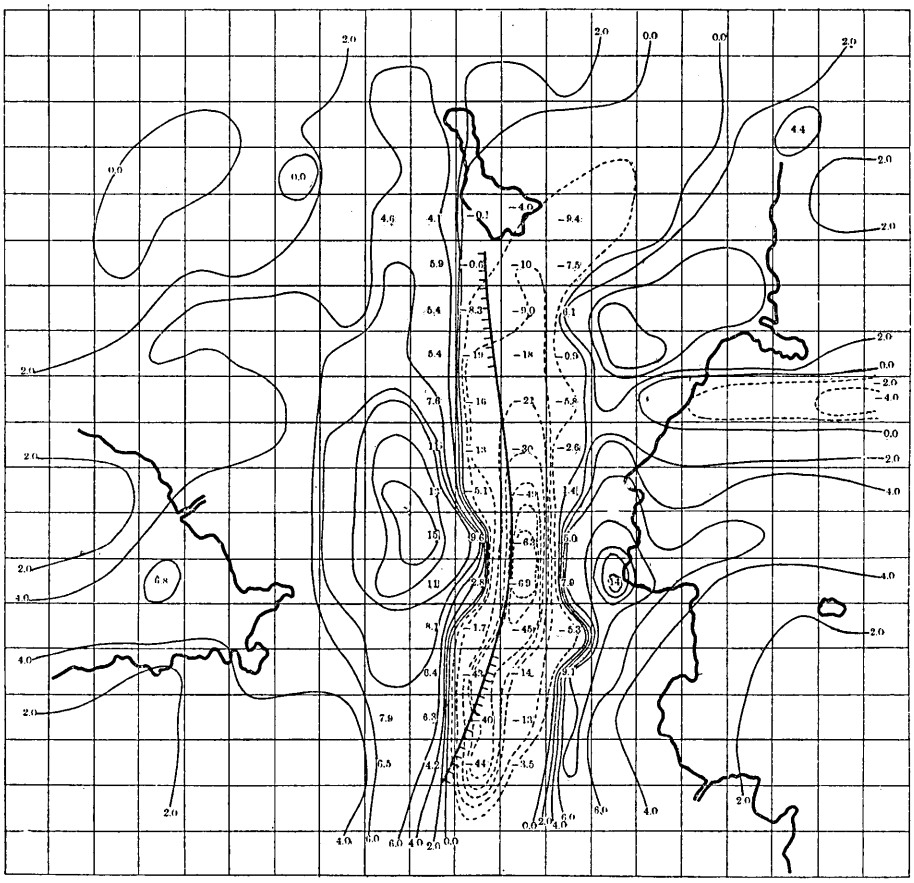

Fig. 5 *b*. Lines of Equal Rotation,

$$\omega=\frac{1}{2}\left(\frac{\partial u}{\partial y}-\frac{\partial v}{\partial x}\right) \text{ in } 10^{-5}.$$

The existence of the Tanna Fault is entirely ignored.

1. Horizontal displacements.

   Case (a). In the NE part of Idu Peninsula, which is situated near the epicentre of the Great Kwantô Earthquake, the dis-

placements which are fairly large, become small with distance from the NE coast above mentioned towards the western region. (see Fig. 1, 15).

Case (*b*). The horizontal displacements, which are generally large on the wide area of these districts, are extremely large in the neighbourhood of the Tanna Fault.

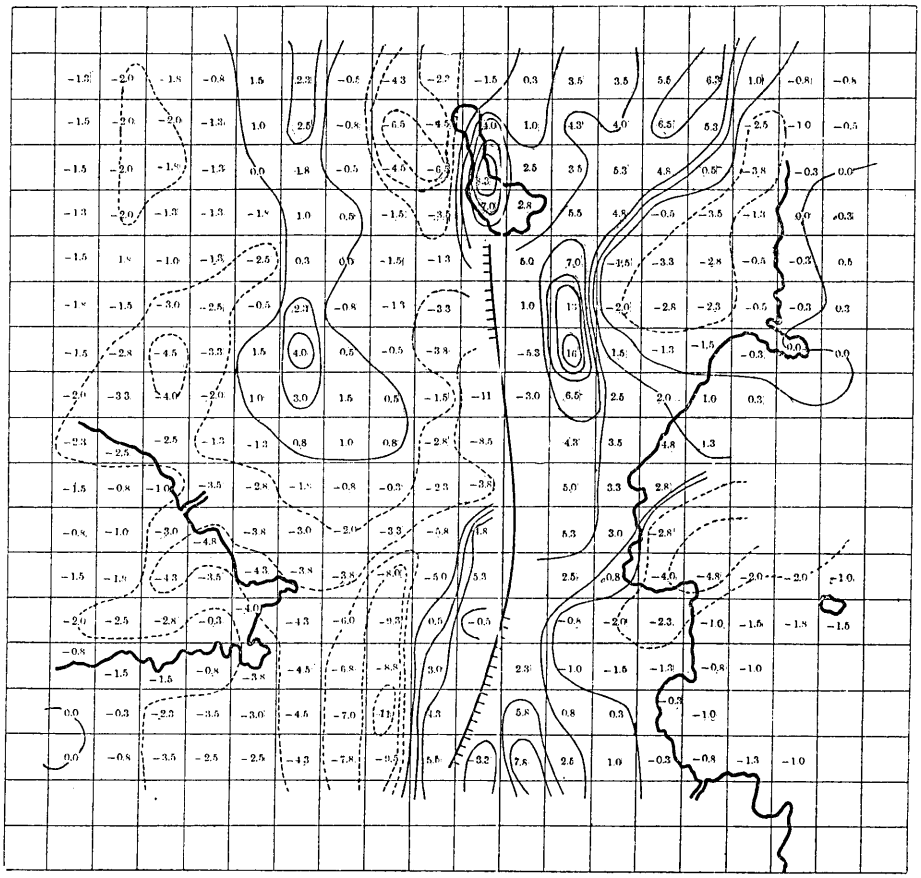

Fig. 6 *a*. Lines of Equal Eastward Gradient of Eastward Displacement, $\frac{\partial u}{\partial x}$, in 10^{-5}.

2. Dilatation.

Case (*a*). Near Atami, and also near Ueno and Isibasi, in the northern regions of Manaduru, as well as near Hasima, there are four conspicuous negative maxima of dilatation. Near the coast, in the middle of Atami and Manaduru, there is a positive

maximum. Near Suwadai and Kamohara, in the SW region of Asinoko, there is a large positive dilatation (see Fig. 3, 16).

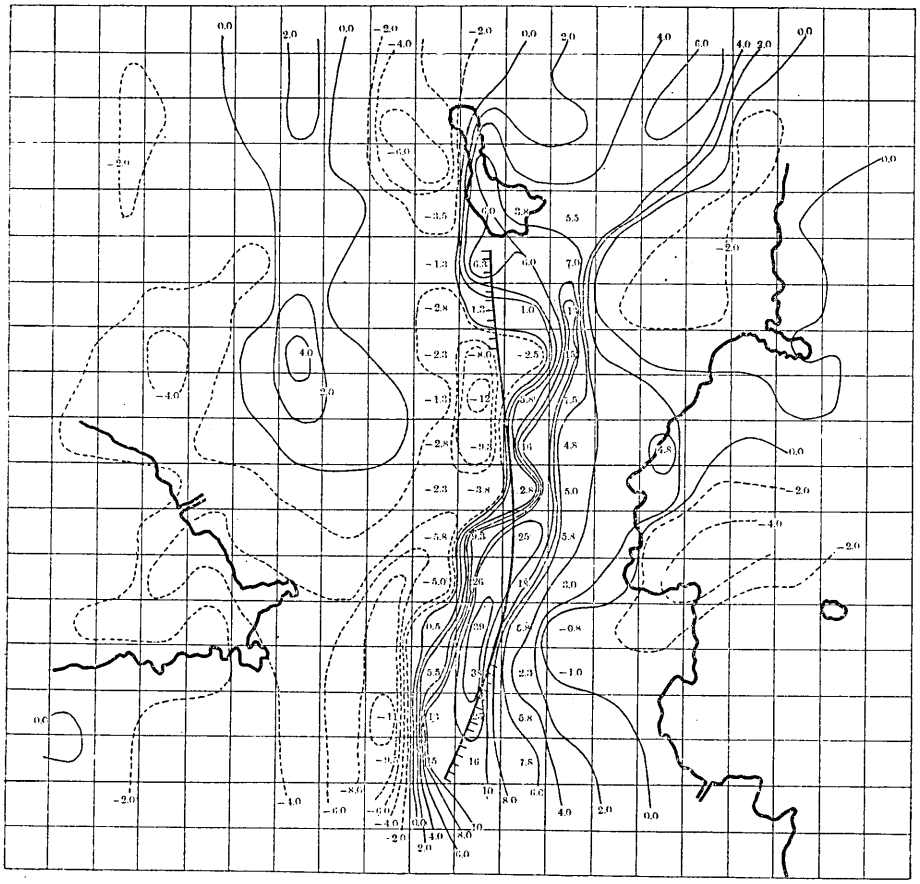

Fig. 6 *b*. Lines of Equal Eastward Gradient of Eastward Displacement, $\frac{\partial u}{\partial x}$, in 10^{-5}. The existence of the Tanna Fault is entirely ignored.

Case (*b*). There are two regions of maximum dilatation at both extremities of the Tanna Fault, the northern one near Asinoko and the southern near Mt. Isigami. Near Ukihasi west of the fault, and also in the middle part on east of the fault, there are *second* maximum dilatations. On the east side of the northern part of the fault, near Miyakami, Karesugi, Minamigô and Ueno, there is a region of negative dilatation.

3. Shear.

Case (*a*). Near Manaduru and in its northern region, there are

positive maxima of shear. From the west of this positive region, above cited, to the region near Atami, there is a large value of negative shear (see Fig. 17).

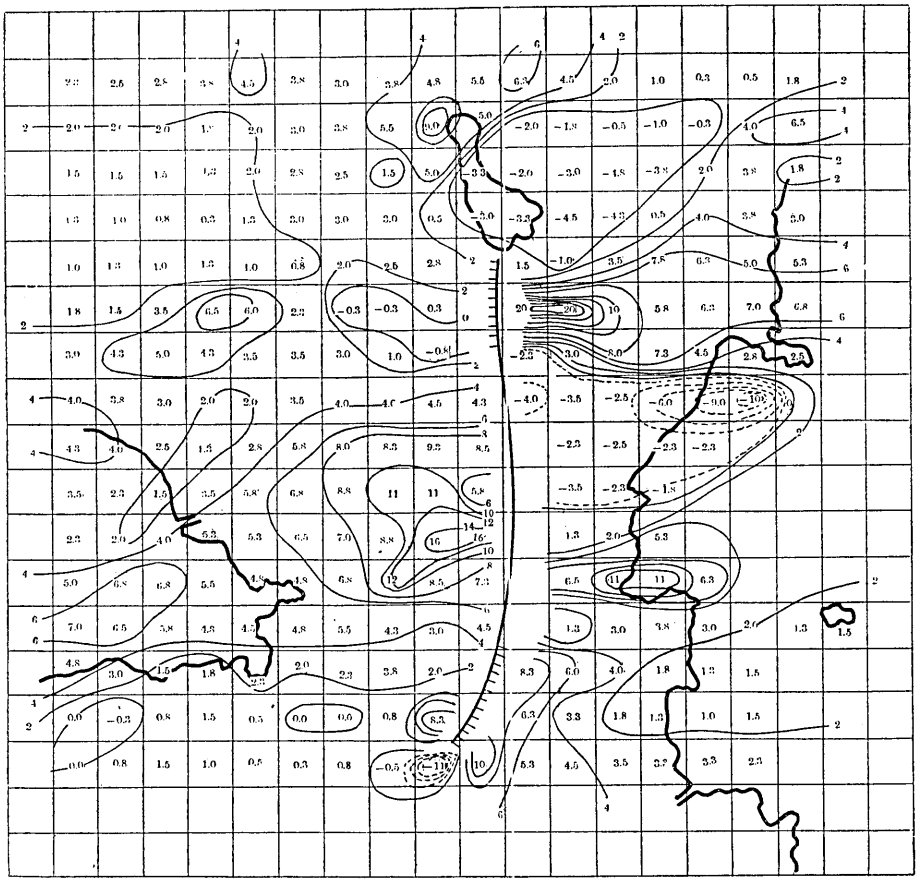

Fig. 7 *a*. Lines of Equal Northward Gradient of Eastward Displacement, $\frac{\partial u}{\partial y}$ in 10^{-5}.

Case (*b*). In Fig. 4, *a*, we see that the maximum regions of positive shear on both extremities are in the east side of the fault, and of negative shear in the middle part of the same side of the fault. In the west side, the maximum value of positive shear is in the middle region, and those of negative shear, on both extremities of the fault, which are on a quite opposite course compared with the east side of the fault.

From Fig. 4, *b*, we see that the shear has its positive

value in the zonal area along the fault, and negative value on both sides of the positive zone. Positively maximum regions exist in the middle and on both extremities of the fault, similar to the preceding case.

4. Rotation.

Case (*a*). Near Atami there exists a positive maximum of rotation, and near Simoaido a negative one. Except this negative

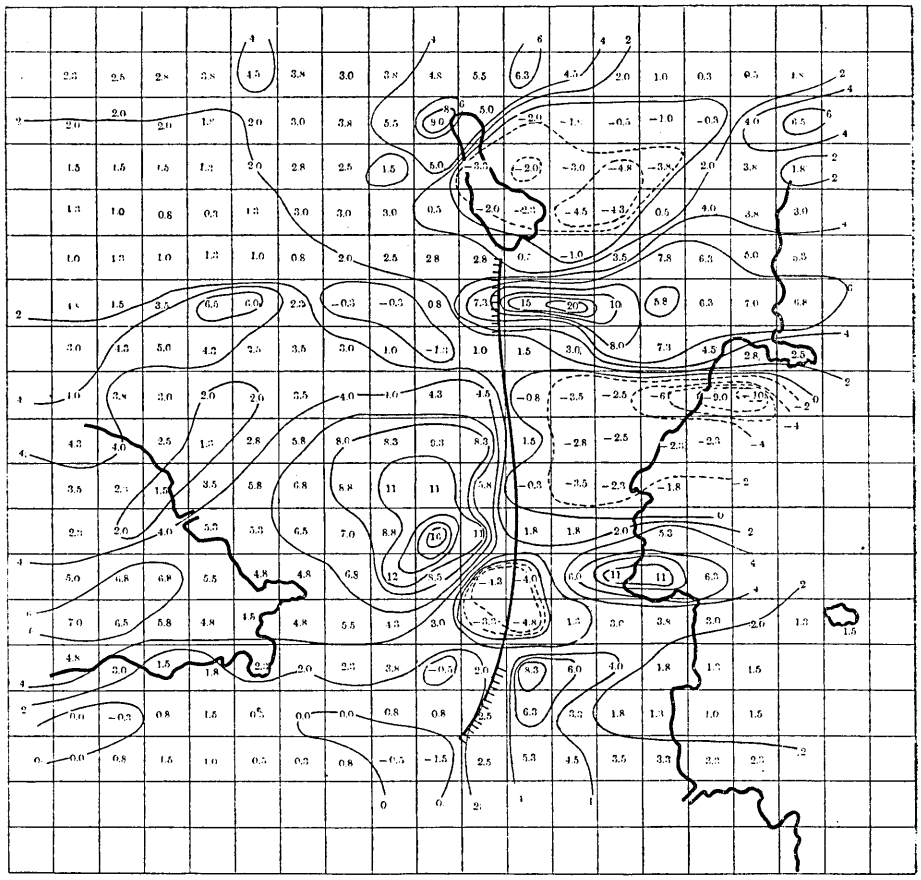

Fig. 7 *b*. Lines of Equal Northward Gradient of Eastward Displacement, $\frac{\partial u}{\partial y}$ in 10^{-5}. The existence of the Tanna Fault is entirely ignored.

maximum region and the negative region of small magnitude near Numatu, the other regions in Idu Peninsula are all of positive rotation (see Fig. 18).

Case (*b*). From Fig. 5, *a*, we see that there are two regions of

maximum positive rotation on each side at about the middle of the fault, and that the area of Idu Peninsula is mostly of positive rotation, except a small area near the northern extremity of the fault, near Asinoko, Kamurigatake, and Isibasi, all of which are of negative rotation.

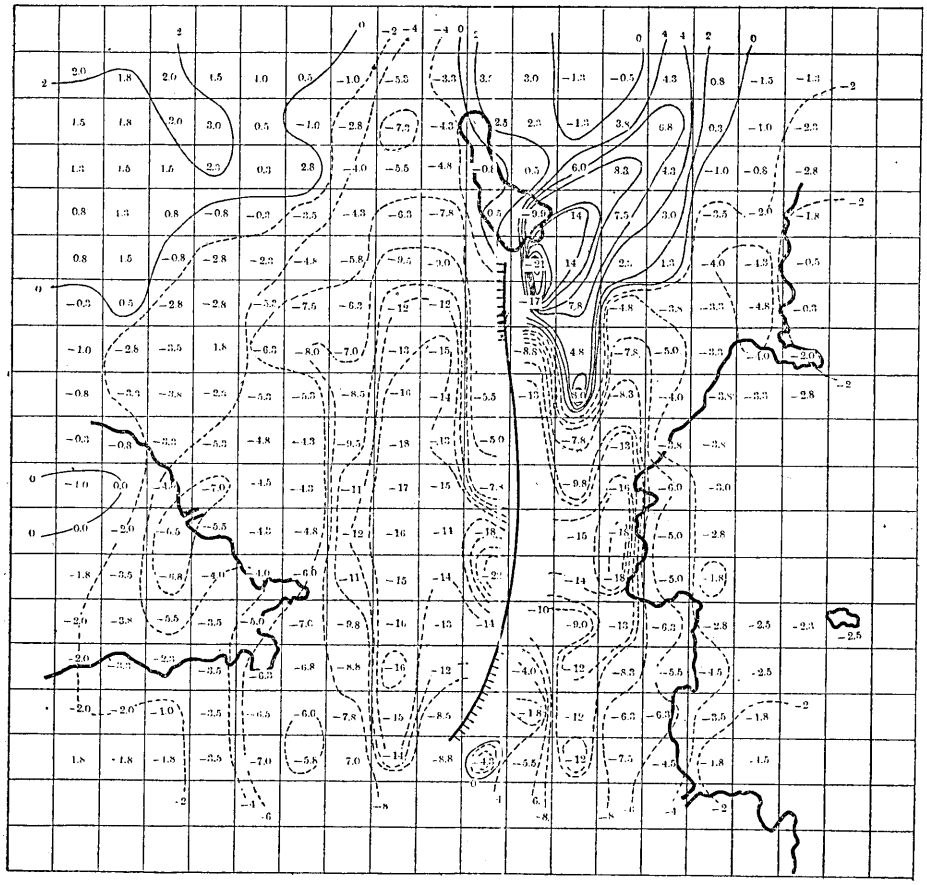

Fig. 8 *a*. Lines of Equal Eastward Gradient of Northward Displacement, $\frac{\partial v}{\partial x}$ in 10^{-5}.

Fig. 5, *b*, shows that the zonal area along the fault is of negative rotation, while on both sides of the zone, we see regions of positive rotation. We also meet with two maximum regions of positive rotation on both sides in the middle part of the fault, similar to the case of Fig. 5, *a*.

5. Maximum Shear.

Case (*a*). Near Minamigô, in the northern region of Manaduru,

and near Atami, as well as near Kamiyama and Suwadai, in the western region of Asinoko, there are large values of maximum shear. Near Hasima also, there is a large value of maximum shear. The northern region of Enasi has a rather large value of maximum shear (see Fig. 19).

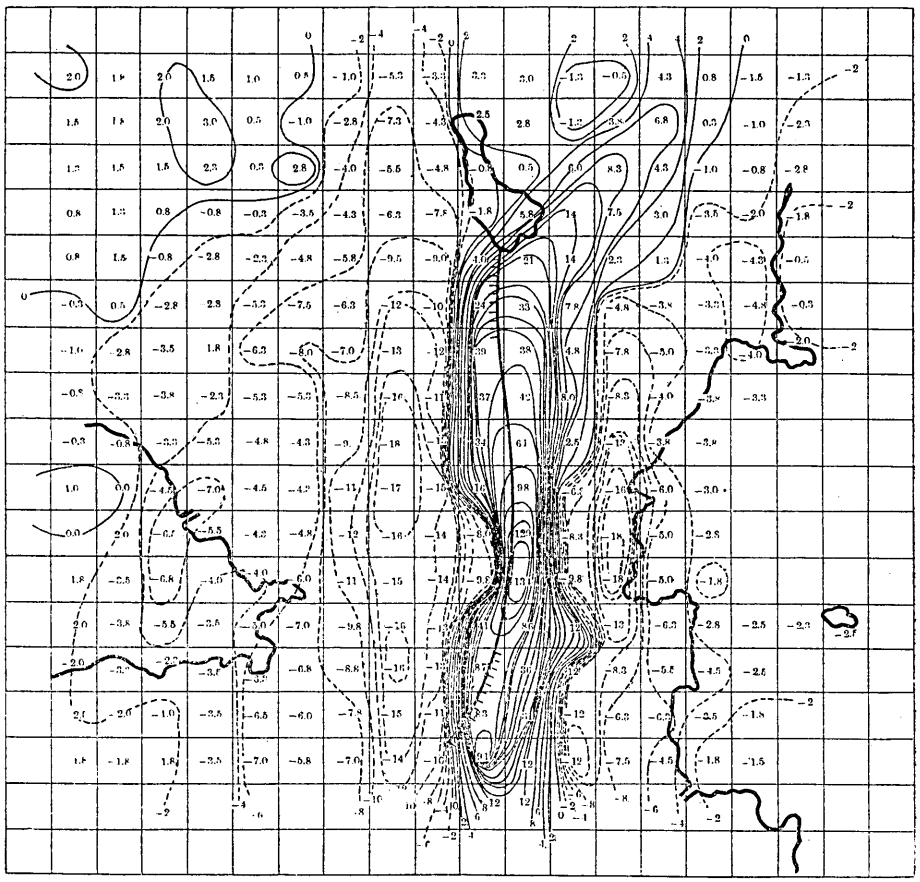

Fig. 8 *b*. Lines of Equal Eastward Gradient of Northward Displacement, $\frac{\partial v}{\partial x}$ in 10^{-5}. The existence of the Tanna Fault is entirely ignored.

Case (*b*). From Fig. 12, *a*, *b*, we see that there are three regions of large values of maximum shear on both extremities, and in the middle part east of the fault, and a region of small value in the middle part west of the fault. These values increase towards the south along the fault.

6. Principal Strain.

Case (a). Similar to the case of the horizontal displacements, large values of principal strains exist in the NE region of the Idu Peninsula, their values gradually diminishing with distance from this region towards the west. Most directions of the principal strains along the NE coast of the Idu Peninsula are inclined about 45° to the coast line (see Fig. 20).

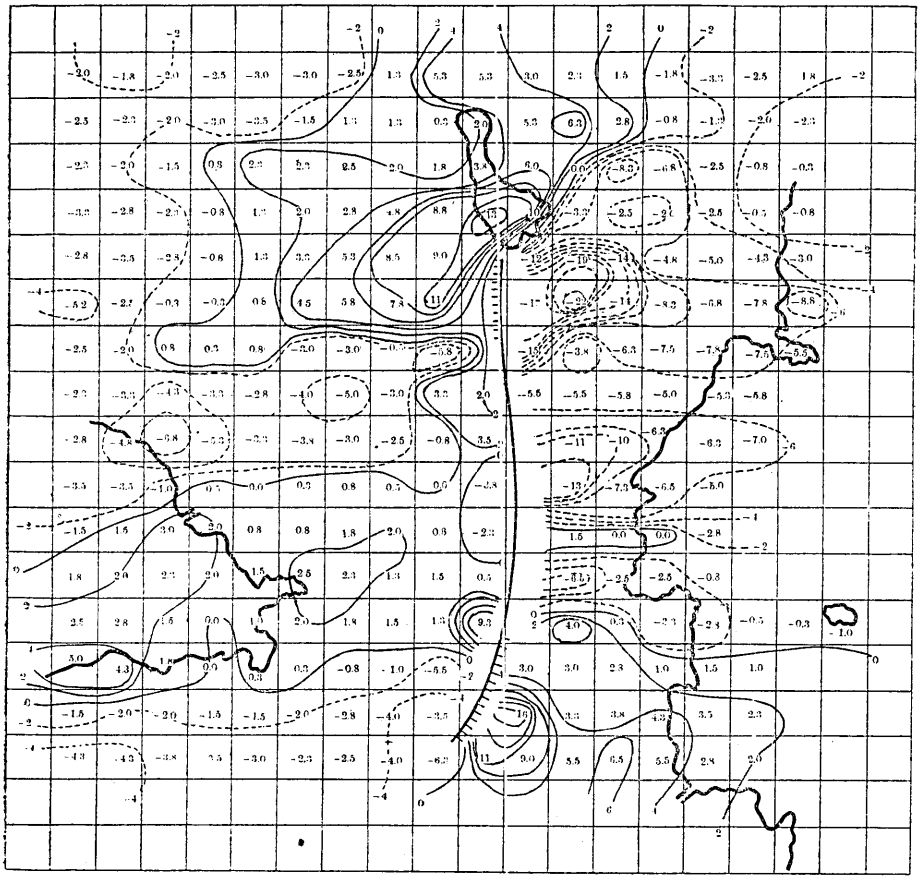

Fig. 9 a. Lines of Equal Northward Gradient of Northward Displacement, $\frac{\partial v}{\partial y}$ in 10^{-5}.

Case (b). In the southern half of the west side along the fault, contraction of the earth's crust took place in direction parallel to the fault, and elongation perpendicular to the fault, approximately. The relation between elongation and contraction against

the fault line is contrary in the northern half of the west side zone compared with the southern half. East of the fault, the principal strains are maximum at both extremities of the fault. In the middle part of the fault, a zone with relatively large strains extends from the fault to the coast of Atami.

(see Fig. 13, *a*).

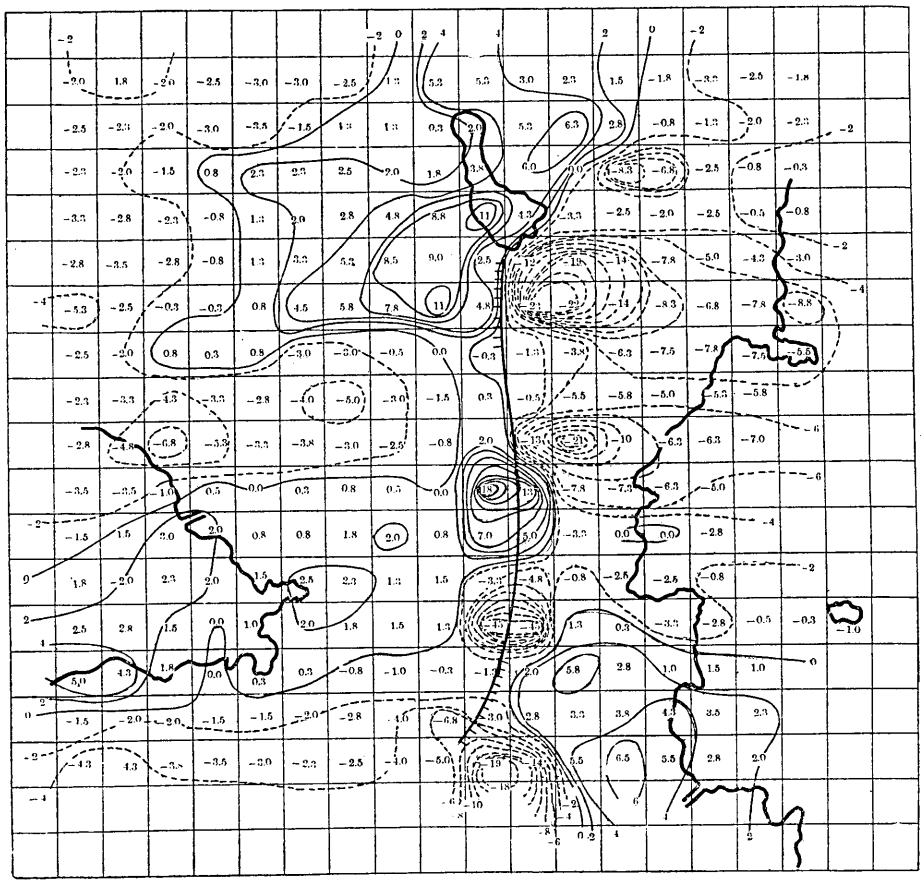

Fig. 9 b. Lines of Equal Northward Gradient of Northward Displacement, $\frac{\partial v}{\partial y}$ in 10^{-5}.

The existence of the Tanna Fault is entirely ignored.

From Fig. 13, *b*, it will be seen that the axes of principal strains are inclined about 45° to the fault line, and that the magnitude of strain increases towards the south from the middle to the southern end of the zone. The amount of strain is usually very small in regions far from the fault.

7. Eastward Gradient of Eastward Displacement $\frac{\partial u}{\partial x}$.

Case (a). A positive maximum of $\frac{\partial u}{\partial x}$ exists near Simoaido, situated not very far from the epicentral region of the Great Kwantô Earthquake, and negative maximum near Isibasi in the neighbourhood of Simoaido. A negative maximum of $\frac{\partial u}{\partial x}$ exists also

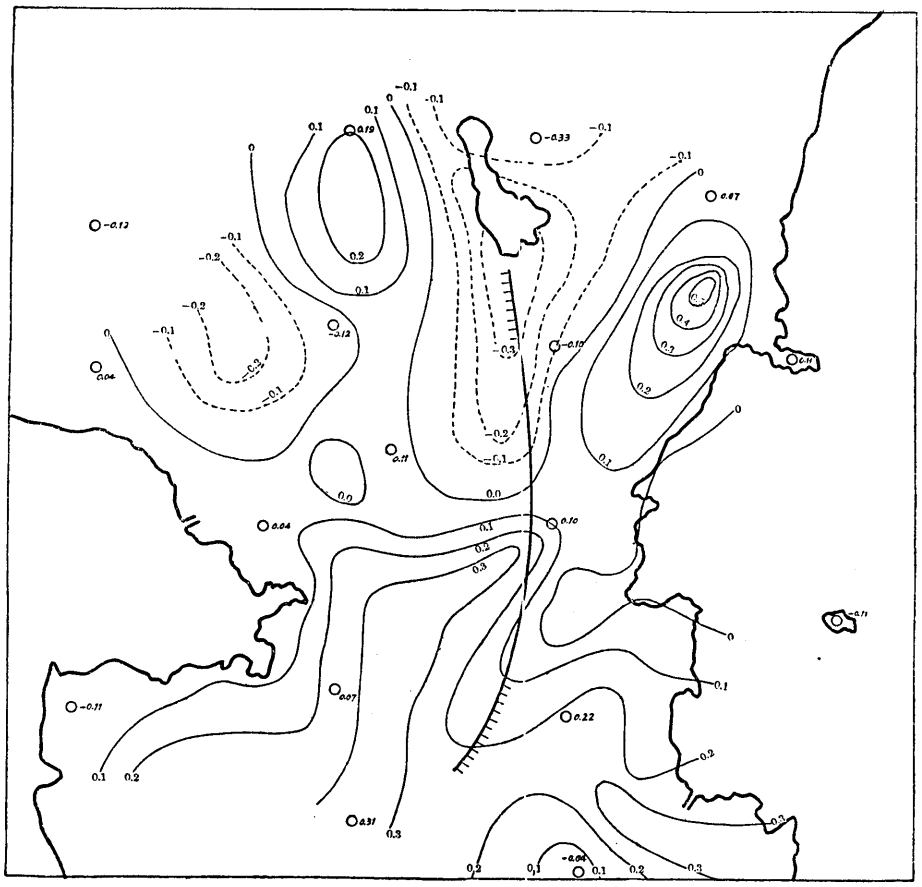

Fig. 10 a. Lines of Equal Vertical Displacement, w, in metre, connected with the Idu Destructive Earthquake.

near Atami, facing, near Hatamura, the positive maximum. Generally speaking, large values of $\frac{\partial u}{\partial x}$ exist along the coast line in the N E region of the Idu Peninsula (see Fig. 21).

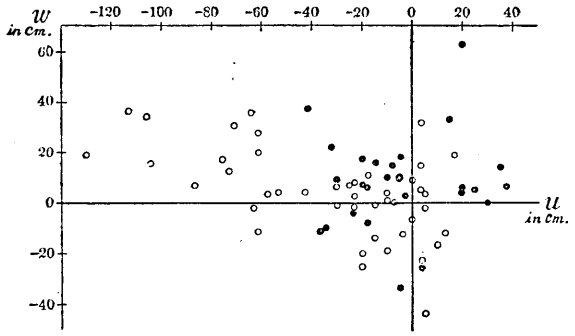

Fig. 10. *b.* $u\ w$-Diagram. ○ marks the station on the west side of the Tanna Fault.

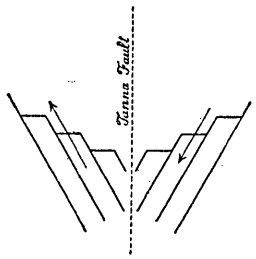

Fig. 11. The Step-Faults.

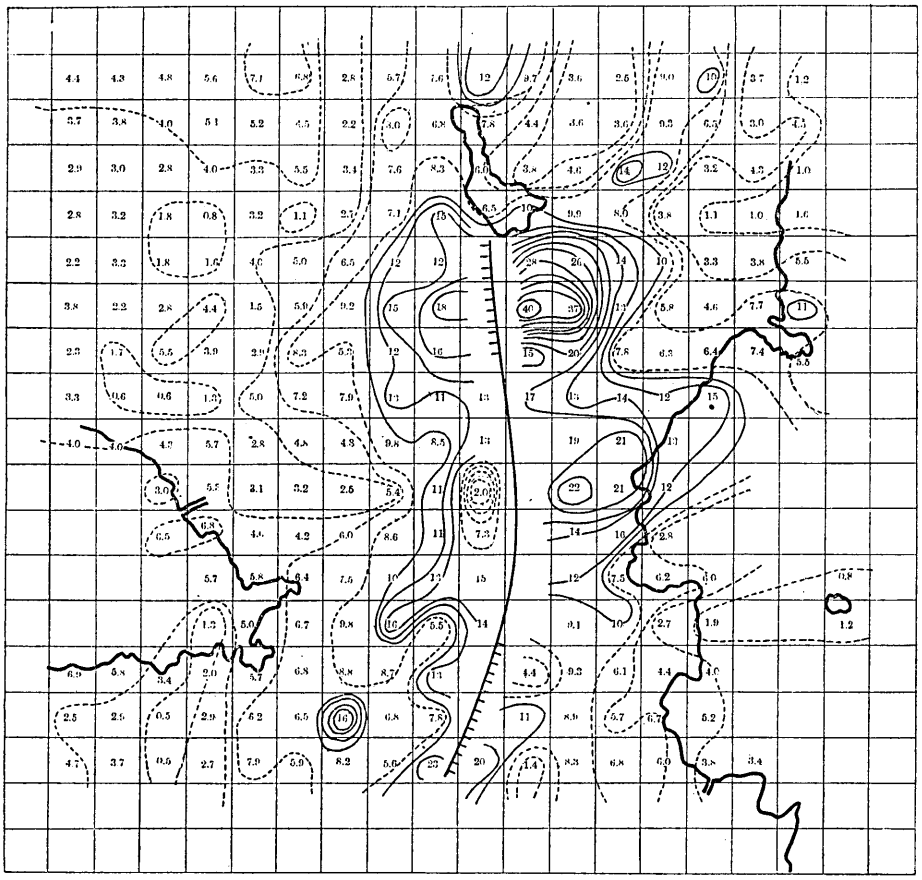

Fig. 12 *a*. Lines of Equal Maximum Shear,

$$\sqrt{\left(\frac{\partial u}{\partial x}-\frac{\partial v}{\partial y}\right)^2+\left(\frac{\partial v}{\partial x}+\frac{\partial u}{\partial y}\right)^2}\ \text{in}\ 10^{-5}.$$

Case (b). About both extremities of the fault, i. e., near Asinoko, Karesugi, and Kunimiisi, as well as about the S W part of the Mt. Sukumo, there are maxima of $\frac{\partial u}{\partial x}$. Near Kuwabara and Hirae, and also near Takyô and Kosaka, there are maxima of $\frac{\partial u}{\partial x}$ (see Fig. 6).

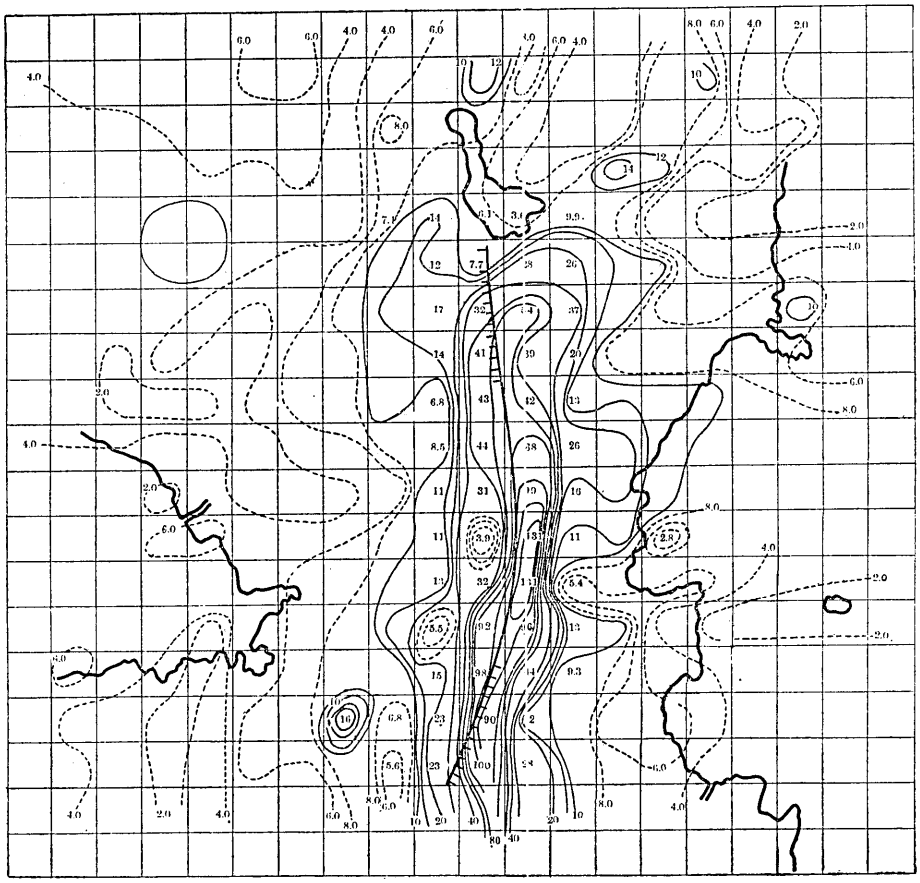

Fig. 12 b. Lines of Equal Maximum Shear,

$$\sqrt{\left(\frac{\partial u}{\partial x}-\frac{\partial v}{\partial y}\right)^2+\left(\frac{\partial v}{\partial x}+\frac{\partial u}{\partial y}\right)^2} \text{ in } 10^{-5}.$$

The existence of the Tanna Fault is entirely ignored.

8. Northward Gradient of Eastward Displacement $\frac{\partial u}{\partial y}$.

Case (a). In the neighbourhood of Simoaido and in the southward region next to it, a conspicuous negative maximum of

$\frac{\partial u}{\partial y}$ exists. In the region near Atami there are positive maxima of $\frac{\partial u}{\partial y}$. In almost the whole of this district we find positive regions of $\frac{\partial u}{\partial y}$.

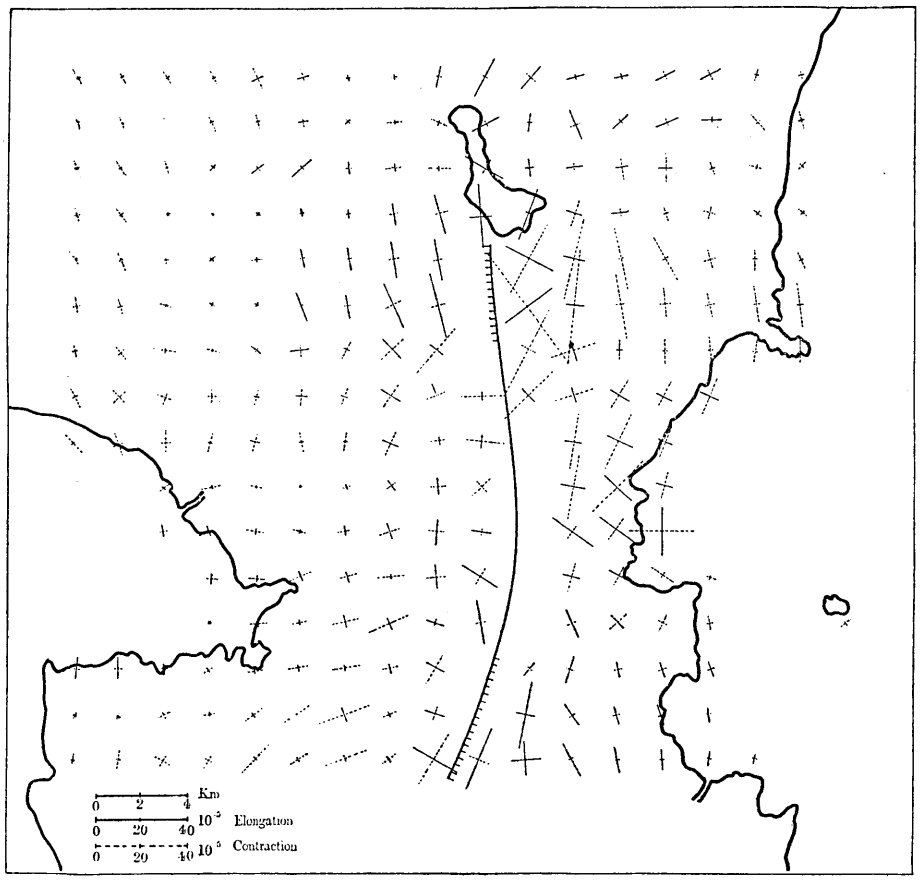

Fig. 13 *a*. Principal Strains,

$$\gamma_{1,2}=\frac{\partial u}{\partial x}+\frac{\partial v}{\partial y}\pm\sqrt{\left(\frac{\partial u}{\partial x}-\frac{\partial v}{\partial y}\right)^2+\left(\frac{\partial v}{\partial x}+\frac{\partial u}{\partial y}\right)^2}.$$

Case (*b*). About the northern extremity of the fault, i. e., near Karesugi, as well as in the middle part west of the fault, near Konaya, there are positive maxima of $\frac{\partial u}{\partial y}$ (see Fig. 7, and 22).

9. Eastward Gradient of Northward Displacement $\frac{\partial v}{\partial x}$.

Case (a). Only the regions near Minamiyosiwara, Nirayama, and Takayama have positive values of $\frac{\partial v}{\partial x}$, nearly all the remainder being regions of negative values. There are negative maxima of $\frac{\partial v}{\partial x}$ along the zonal area running from the northern region to the southern, through the coast of Atami.

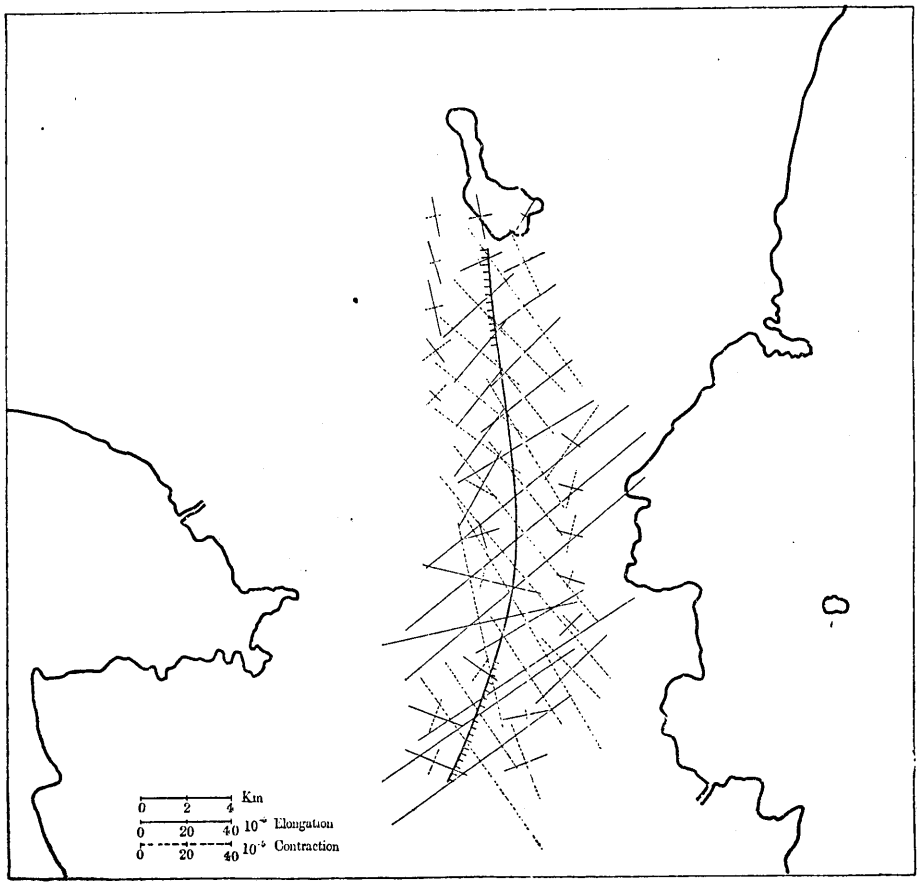

Fig. 13 b. Principal Strains,

$$\gamma_{1,2}=\frac{\partial u}{\partial x}+\frac{\partial v}{\partial y}\pm\sqrt{\left(\frac{\partial u}{\partial x}-\frac{\partial v}{\partial y}\right)^2+\left(\frac{\partial v}{\partial x}+\frac{\partial u}{\partial y}\right)^2}.$$

The existence of the Tanna Fault is entirely ignored.

Case (b). About both extremities of the fault and east of it are conspicuous positive maxima of $\frac{\partial v}{\partial x}$. In the other regions nega-

tive values predominate over a wide area, their maxima being along the fault and also in the region near Atami (see Fig. 8, 23).

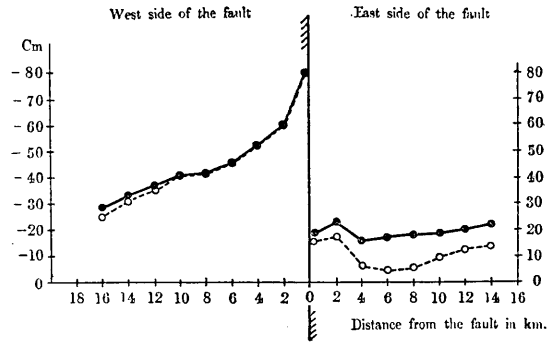

Fig. 14. Absolute (full line), and Algebraic (dotted line) mean of the Quantities.
a. Eastward Displacement, u in cm.

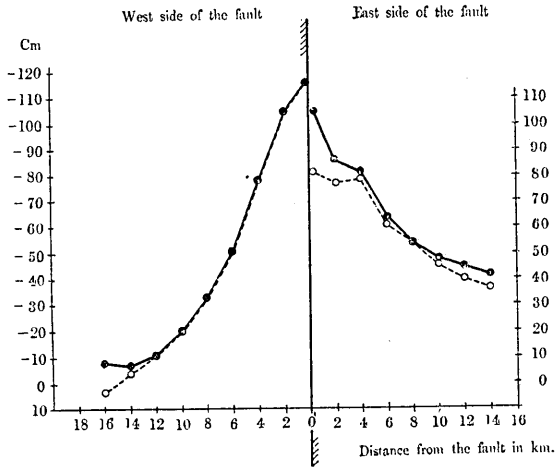

Fig. 14 *b*. Northward Displacement, v in cm.

10. Northward Gradiont of Northward Displacement $\frac{\partial v}{\partial y}$.

Case (*a*). In the N E region of Idu Penidsula, along Sagami Bay, are 3 positive and 3 negative maxima of $\frac{\partial v}{\partial y}$, alternatively. In the western part of Idu Peninsula a positive maximum of $\frac{\partial v}{\partial y}$ exists near Tokukurayama, and near Hasima a negative maximum.

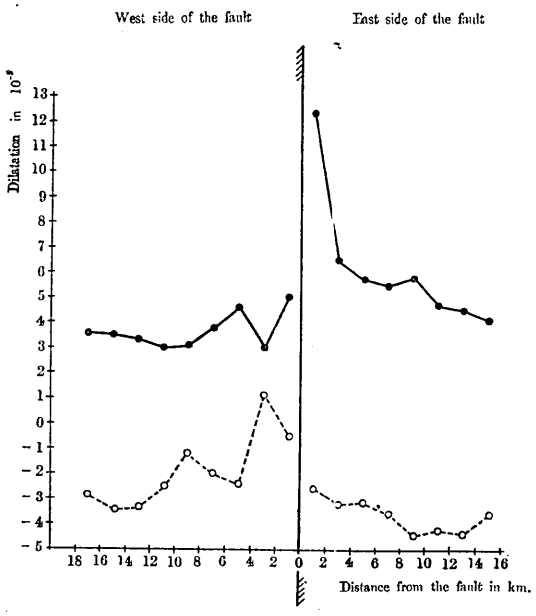

Fig. 14 *c*. Dilatation in 10^{-5}.

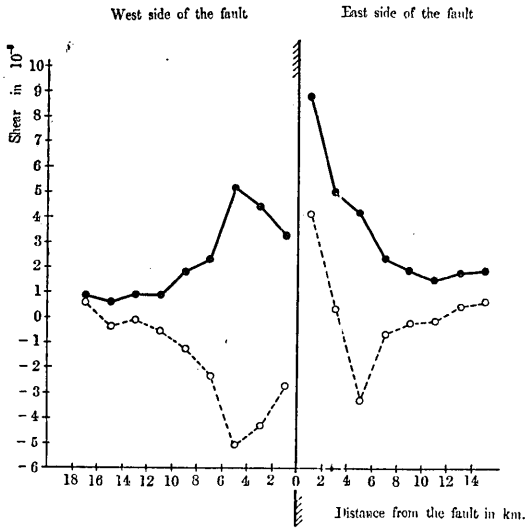

Fig. 14 *d*. Shear in 10^{-5}.

Case (*b*). About the extremities of the fault are positive maxima of $\frac{\partial v}{\partial y}$. On the east side along the fault are some negatively large values of $\frac{\partial v}{\partial y}$ (see Fig. 9, 24).

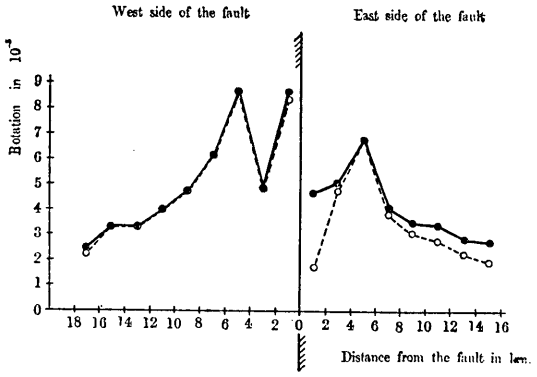

Fig. 14 *e*. Rotation in 10^{-5}.

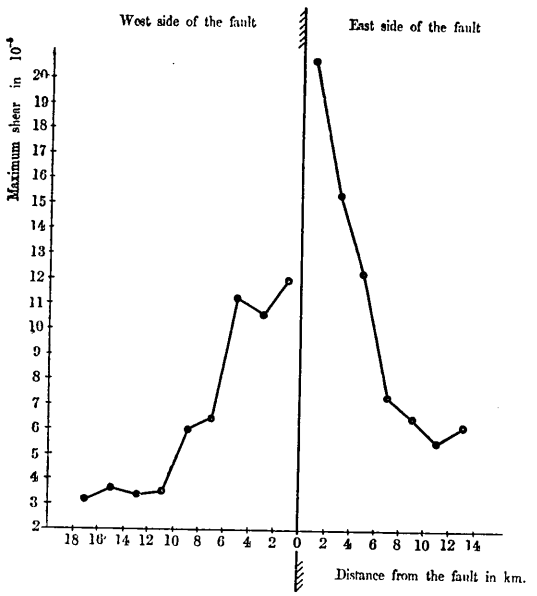

Fig. 14 *f*. Maximum Shear in 10^{-5}.

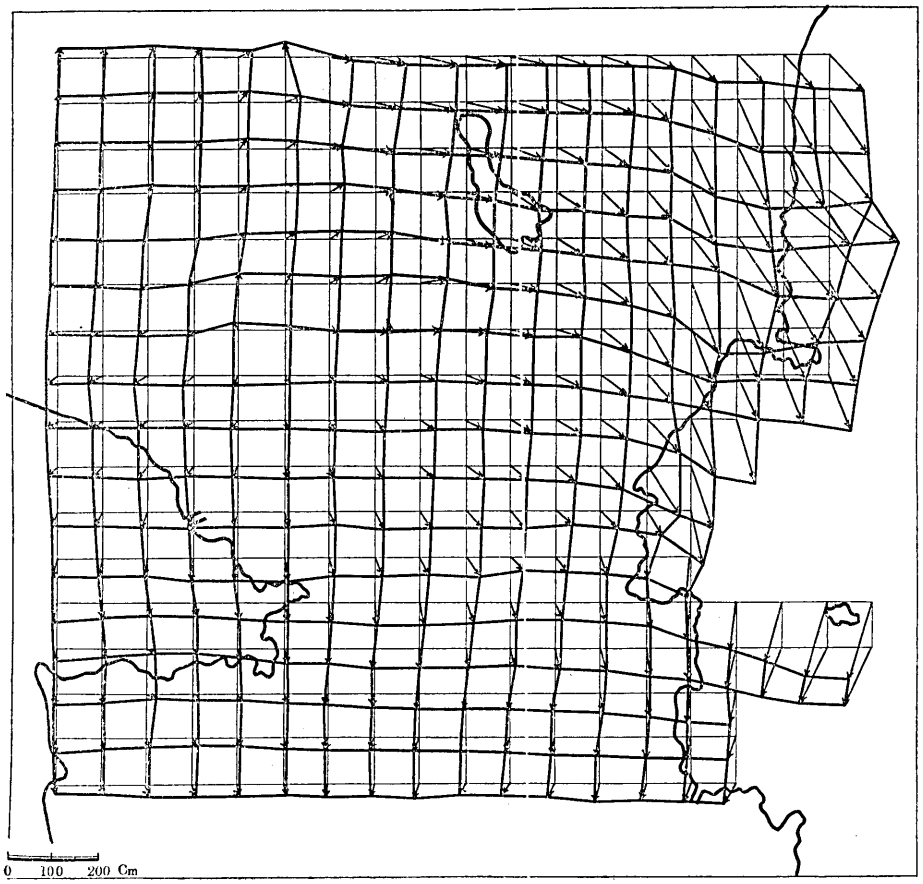

Scale for Displacements.

Fig. 15. Horizontal Displacements of the Mesh-Points, connected with the Great Kwantô Earthquake.

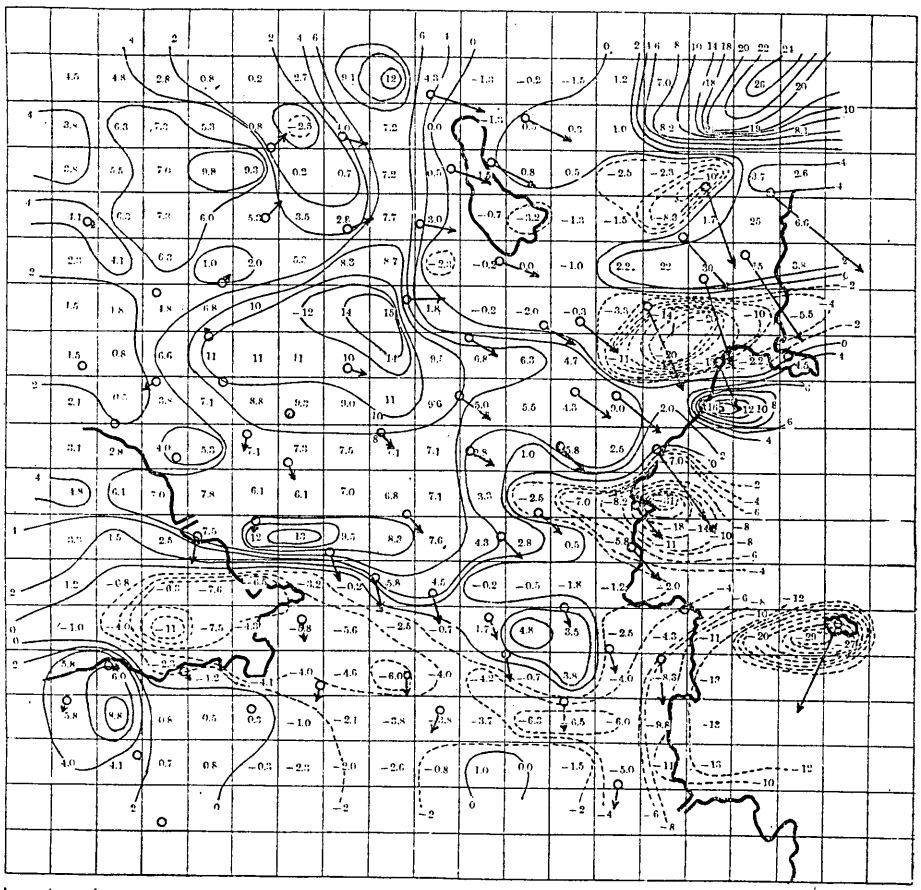

Fig. 16. Lines of Equal Dilatation, $\Delta = \frac{\partial u}{\partial x} + \frac{\partial v}{\partial y}$ in 10^{-5}, connected with the Great Kwantô Earthquake. Arrows show the horizontal displacements of the Triangulation Points.

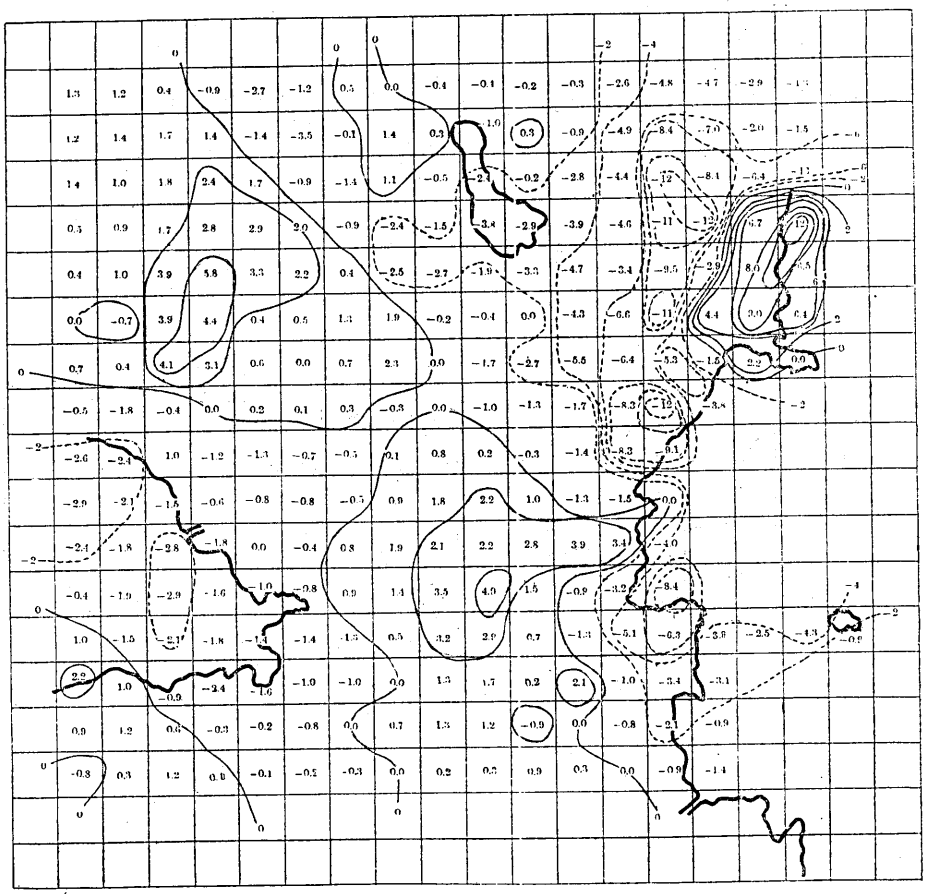

Fig. 17. Lines of Equal Shear, $\sigma=\frac{1}{2}\left(\frac{\partial u}{\partial y}+\frac{\partial v}{\partial x}\right)$ in 10^{-5}, connected with the Great Kwantô Earthquake.

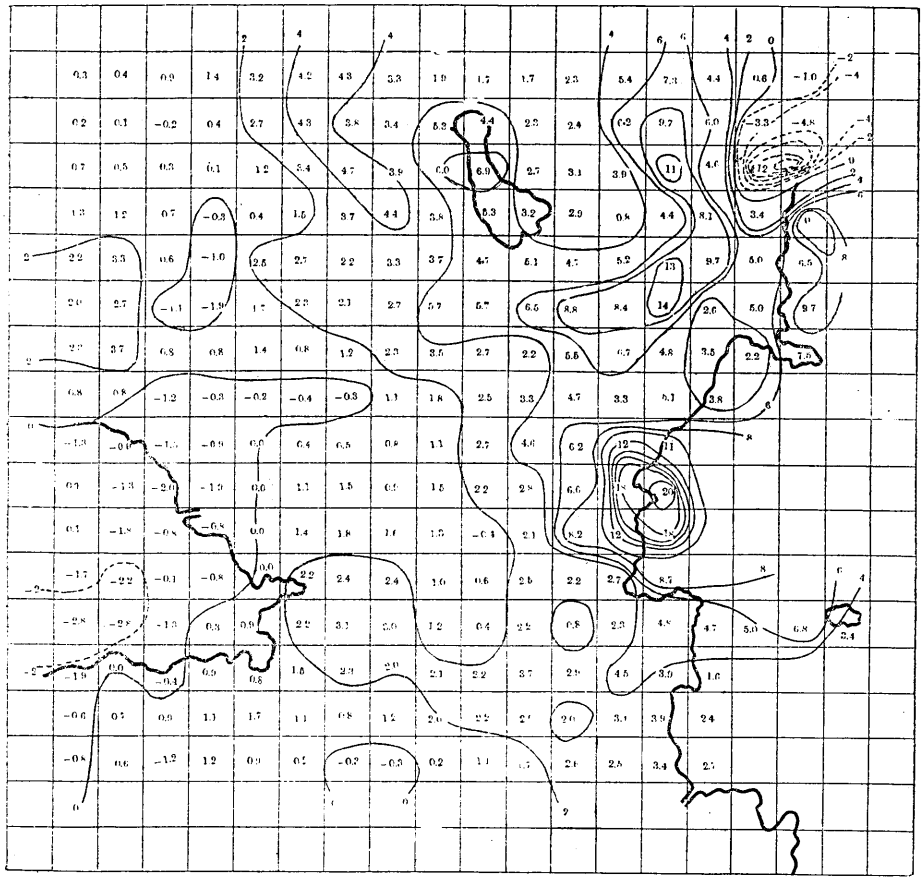

Fig. 18. Lines of Equal Rotation, $\omega=\frac{1}{2}\left(\frac{\partial u}{\partial y}-\frac{\partial v}{\partial x}\right)$ in 10^{-5}, connected with the Great Kwantô Earthquake.

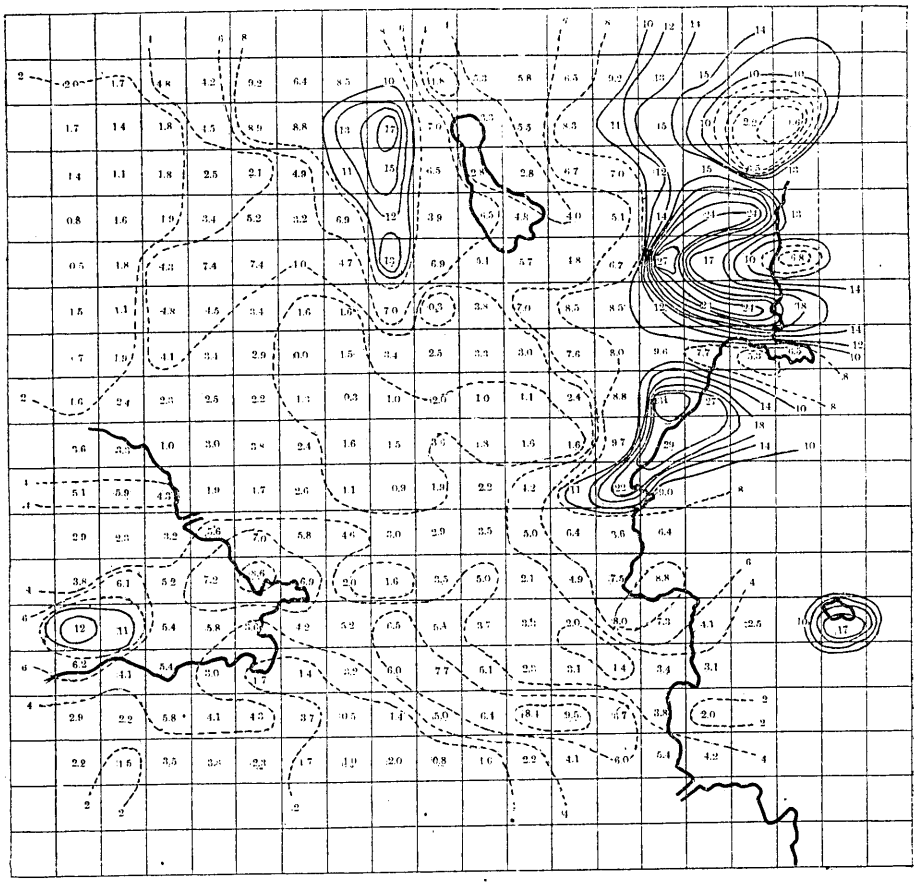

Fig. 19. Lines of Equal Maximum Shear, $\sqrt{\left(\frac{\partial u}{\partial x}-\frac{\partial v}{\partial y}\right)^2+\left(\frac{\partial v}{\partial x}+\frac{\partial u}{\partial y}\right)^2}$ in 10^{-5}, connected with the Great Kwantô Earthquake.

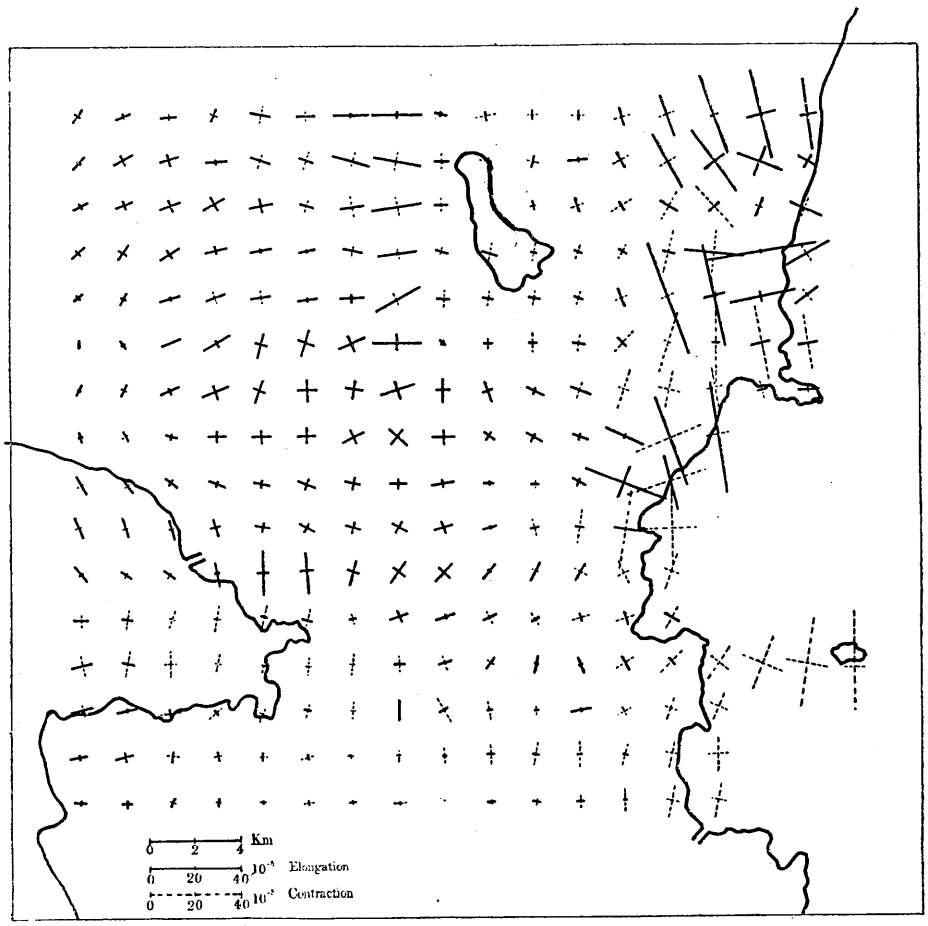

Fig. 20. Principal Strains, $\gamma_{1,2}=\left(\frac{\partial u}{\partial x}+\frac{\partial v}{\partial y}\right)\pm\sqrt{\left(\frac{\partial u}{\partial x}-\frac{\partial v}{\partial y}\right)^2+\left(\frac{\partial v}{\partial x}+\frac{\partial u}{\partial y}\right)^2}$, connected with the Great Kwantô Earthquake.

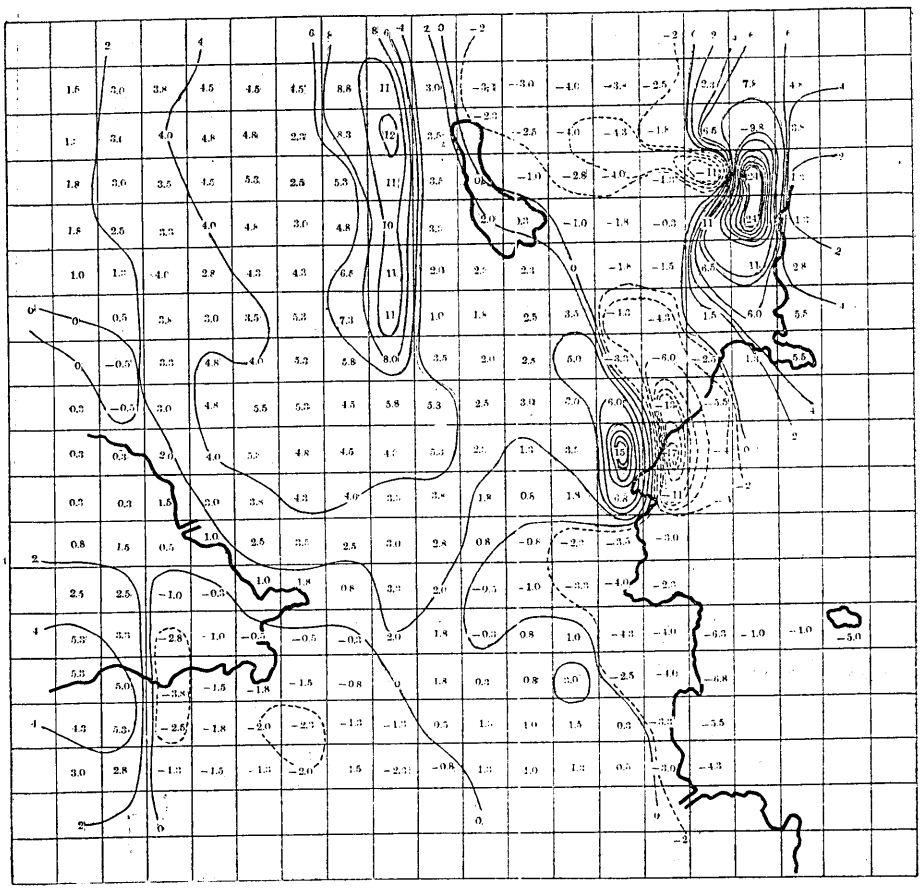

Fig. 21. Lines of Equal Eastward Gradient of Eastward Displacement, $\frac{\partial u}{\partial x}$ in 10^{-5}, connected with the Great Kwantô Earthquake.

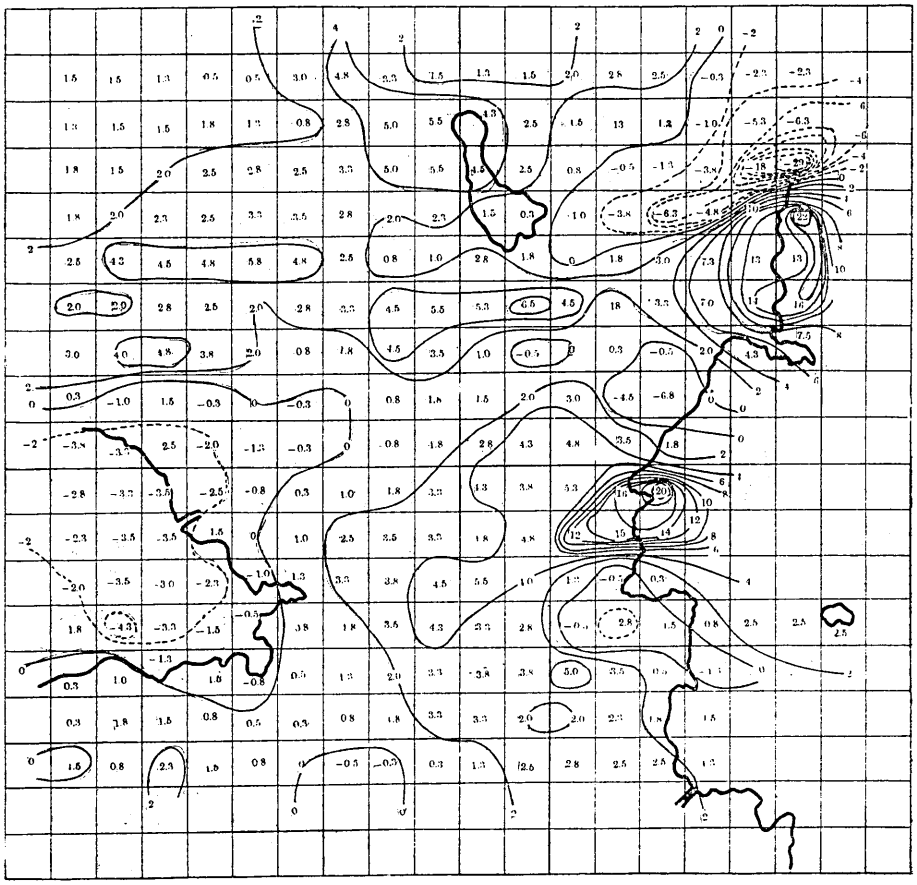

Fig. 22. Lines of Equal Northward Gradient of Eastward Displacement, $\frac{\partial u}{\partial y}$ in 10^{-5}, connected with the Great Kwantô Earthquake.

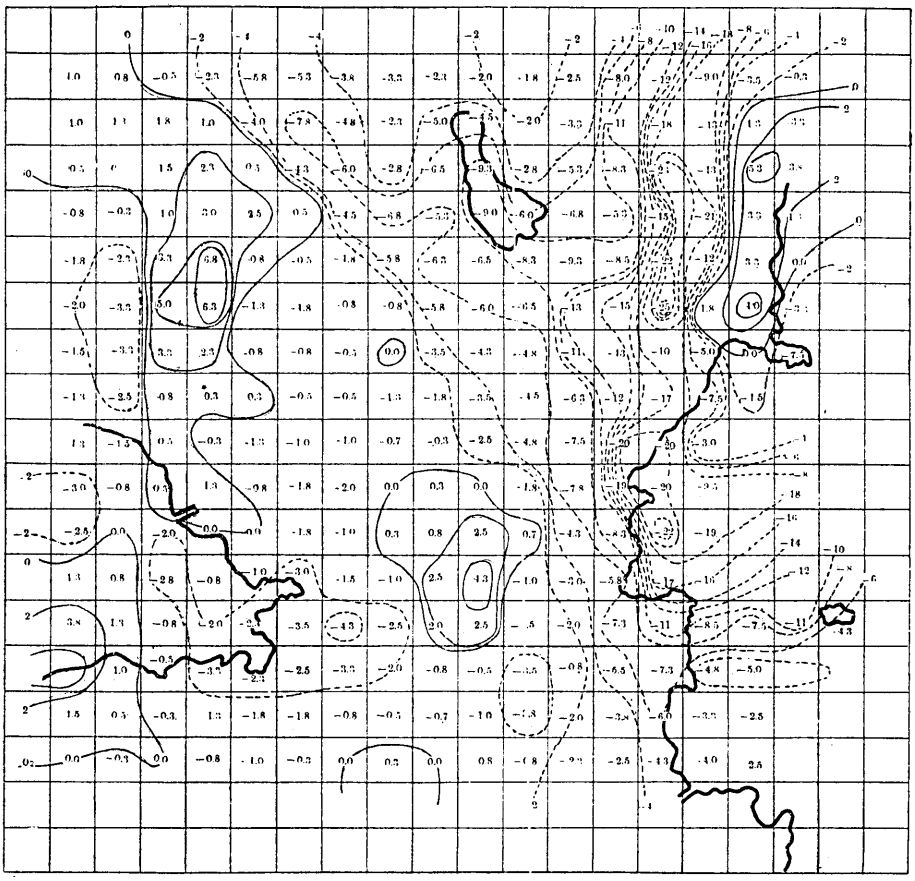

Fig. 23. Lines of Equal Eastward Gradient of Northward Displacement, $\frac{\partial v}{\partial x}$ in 10^{-5}, connected with the Great Kwantô Earthquake.

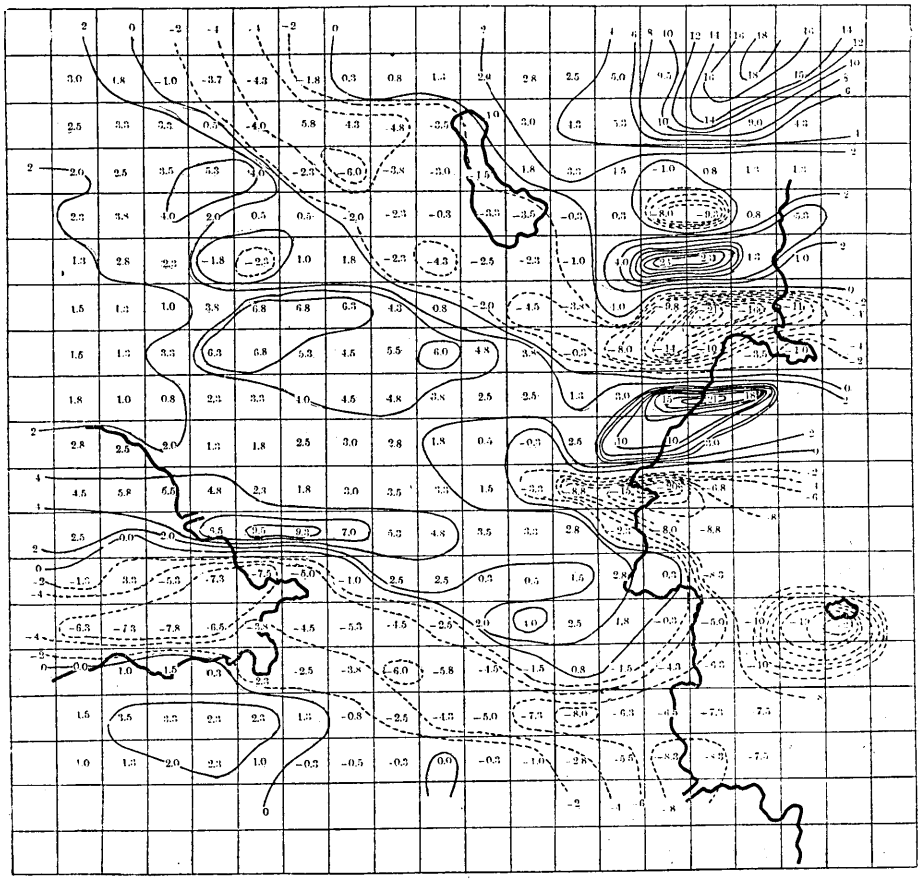

Fig. 24. Lines of Equal Northward Gradient of Northward Displacement, $\frac{\partial v}{\partial y}$ in 10^{-5}, connected with the Great Kwantô Earthquake.

In conclusion, I wish to express may best thanks to Dr. Chûji, Tsuboi, who has given me many useful suggestions in the course of these studies.

---

56. 昭和5年11月26日の北伊豆裂震に伴へる同地方の地殻變動

地震研究所 山口生知

此の伊豆地方の地殻變動の問題は，既に坪井忠二博士に依つて研究された．然し當時は僅かに13點の二等三角測量の結果しか利用し得なかつた．

今回の論文の目的は，其後陸地測量部の力に依つて計測された 71 點の三等三角測量の材料を借用して，更に詳細なる調査を試みることにあつた．尚ほ又地殻の鉛直變動と水平移動との間に何か或る物理學的關係を見出さんことを望んだ．

其の結果は第1圖乃至第 14 圖に示されてゐるがその中の一二を擧ぐれば次の通りである．

丹那斷層の西側に於いては，鉛直變動量 w と東方への水平移動量 u との間には負の相關關係があり，丹那斷層の東側に於ては餘り判然とはしないが正の相關關係がある樣に思はれる．此の u と w との間の關係は第 11 圖に示す如く丹那斷層を境界として階段的地塊層 (Step-faults) の存在を考へることによつて說明されると思ふ．

今回計算した地殻變動を表はす諸量の絕對値は概ね丹那斷層附近に於て最大にして之より遠ざかるに從つて次第に減少してゐる．但し Rotation と Shear のみは斷層線より約 6 km を隔てた地域に於いても著しき最大値を有してゐる．一般に丹那斷層線に於いては，單に水平移動量 u, v のみならず他の諸量も不連續にして而も此の線を境界として，東西對稱性を有してゐないのは著しい事實と思ふ．

尚大正十二年九月一日の關東大地震によつて誘起されたと思はれる地殻變動に就いても同樣の調査を行つて見た．その結果は第 15 圖及至第 24 圖に示される通りである．此の場合は鉛直變動量 w と東への水平變動量，u との間には何等判然たる相關々係の存在を發見し得なかつた．又丹那斷層の如きも判然とは現れて居らない．而して伊豆地震の場合には大なる變動は主として丹那斷層附近に起つて居るが，關東地震の場合には震源地に近き伊豆東北部相模灣沿岸に沿ふて最も大なる變動が起つて居ることが分明となつた．